Supplementary material: SYNERGISTIC INHIBITION OF SARS-COV-2 CELL ENTRY BY OTAMIXABAN AND COVALENT PROTEASE INHIBITORS: PRE-CLINICAL ASSESSMENT OF PHARMACOLOGICAL AND MOLECULAR PROPERTIES

Tim Hempel[1,2,†], Katarina Elez[1,†], Nadine Krüger[3,†], Lluís Raich[1], Jonathan H. Shrimp[4], Olga Danov[5], Danny Jonigk[5,6], Armin Braun[5], Min Shen[4], Matthew D. Hall[4], Stefan Pöhlmann[3,7], Markus Hoffmann[3,7], and Frank Noé[1,2,8,*]

[1]Department of Mathematics and Computer Science, Freie Universität Berlin, Berlin, Germany
[2]Department of Physics, Freie Universität Berlin, Berlin, Germany
[3]Infection Biology Unit, German Primate Center – Leibniz Institute for Primate Research, Göttingen, Germany
[4]National Center for Advancing Translational Sciences, National Institutes of Health, Rockville, MD, USA
[5]Fraunhofer Institute for Toxicology and Experimental Medicine (ITEM), Biomedical Research in Endstage and Obstructive Lung Disease Hannover (BREATH), Member of the German Center for Lung Research (DZL), Member of Fraunhofer International Consortium for Anti-Infective Research (iCAIR), Hannover, Germany
[6]Institute of Pathology, Hannover Medical School, Biomedical Research in Endstage and Obstructive Lung Disease Hannover (BREATH), Hannover, Germany
[7]Faculty of Biology and Psychology, University Göttingen, Göttingen, Germany
[8]Department of Chemistry, Rice University, Houston, TX, USA

† Equal contribution
* Corresponding author: frank.noe@fu-berlin.de

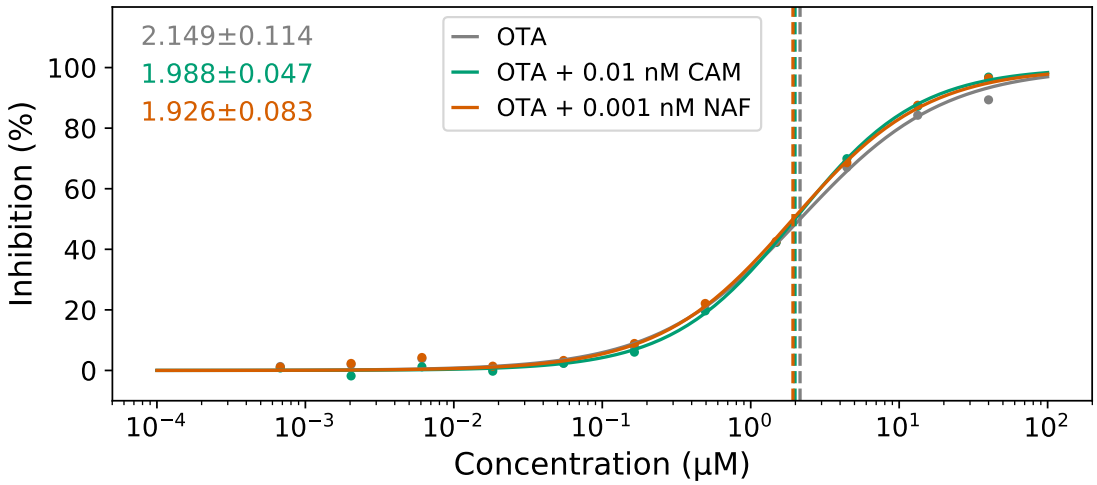

Figure S1: Dose-response curves with their respective IC50 estimates in NIH/NCATS high throughput screening assay (room temperature, one replicate).

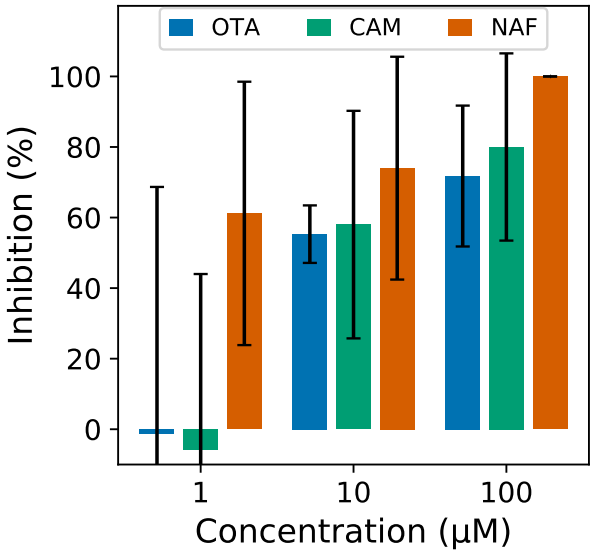

Figure S2: Repetition of PCLS experiment with samples from independent second donor. Inhibition of SARS-CoV-2 infection by otamixaban (blue), camostat (green) and nafamostat (orange) in precision cut human lung slices (PCLS). The results (mean) of three technical replicates are shown. Error bars indicate SD.

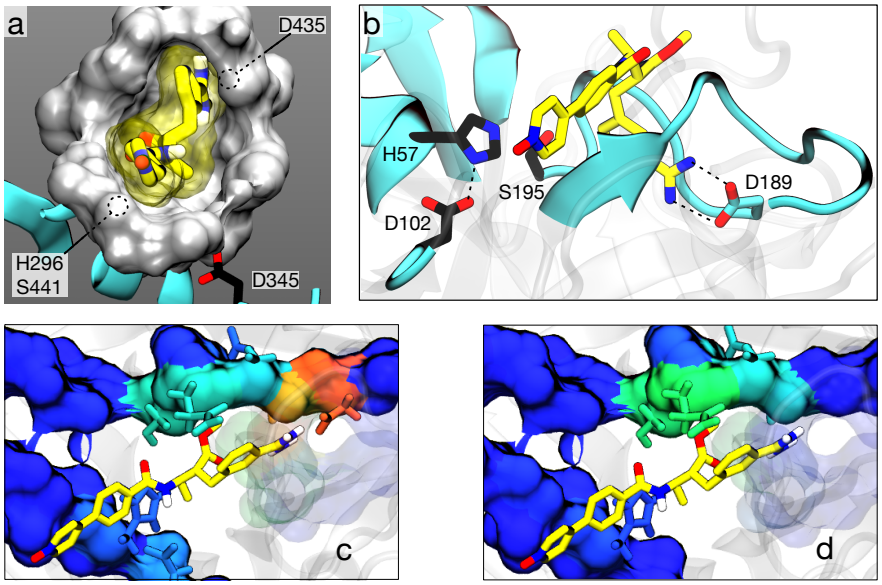

Figure S3: **(a)** Otamixaban (yellow) in the TMPRRS2 binding scaffold (grey surface). Protein surface is restricted to atoms within 0.5 nm range of the drug. Structure is a representative of the most populated MD state. **(b)** Otamixaban in crystal configuration with Human Coagulation Factor Xa (PDB ID: 1KSN [1]). Residue color code as corresponding to TMPRSS2 sequence. **(c+d)** Contact frequencies with benzamidine moiety **(c)** and methyl-esther **(d)**, respectively.

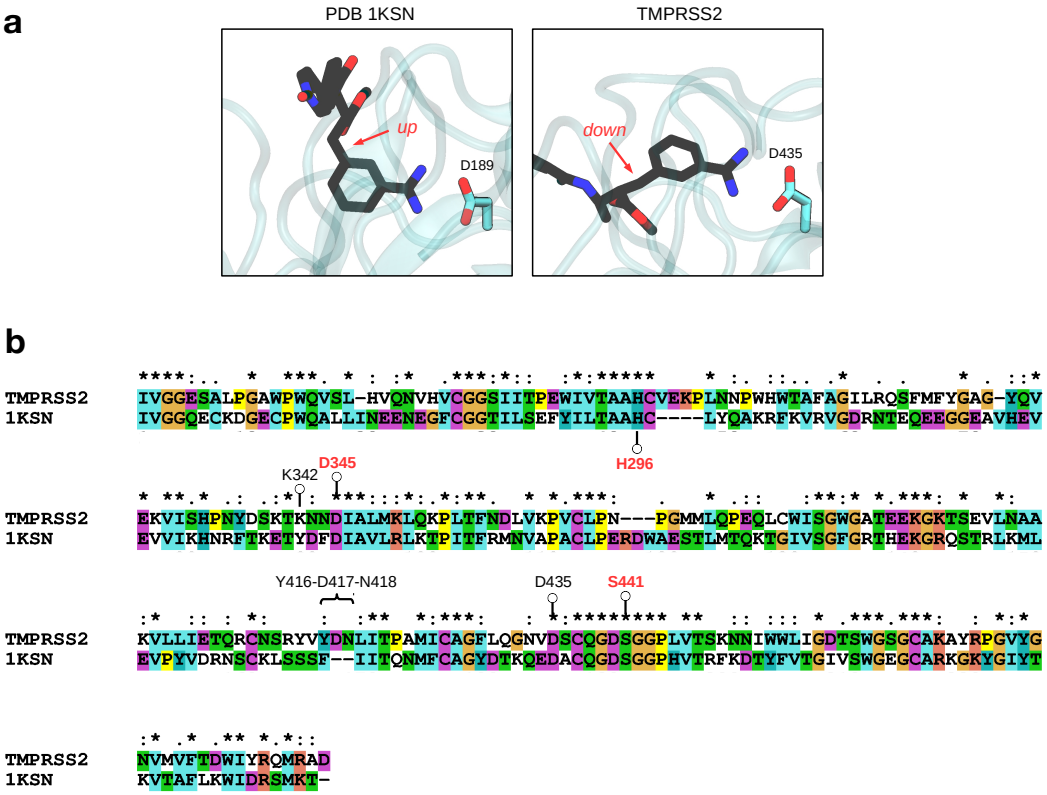

Figure S4: **(a)** Binding mode of otamixaban in the coagulation factor Xa (PDB 1KSN) and in our TMPRSS2 model. Note that in both cases the benzamidine moiety is in the S1 pocket interacting with the conserved aspartate, but the orientation of the molecule is flipped along the axis that goes through the benzene ring and the amidinium group. **(b)** Sequence alignment highlighting the catalytic triad in red. Note the differences at positions K342 and Y416-N418 (TMPRSS2 numbering) involved in interactions with the pyridine-N-oxide moiety in PDB 1KSN. The alignment was done with MUSCLE v3.8 [2] and the image with Clustal X 2.1 [3].

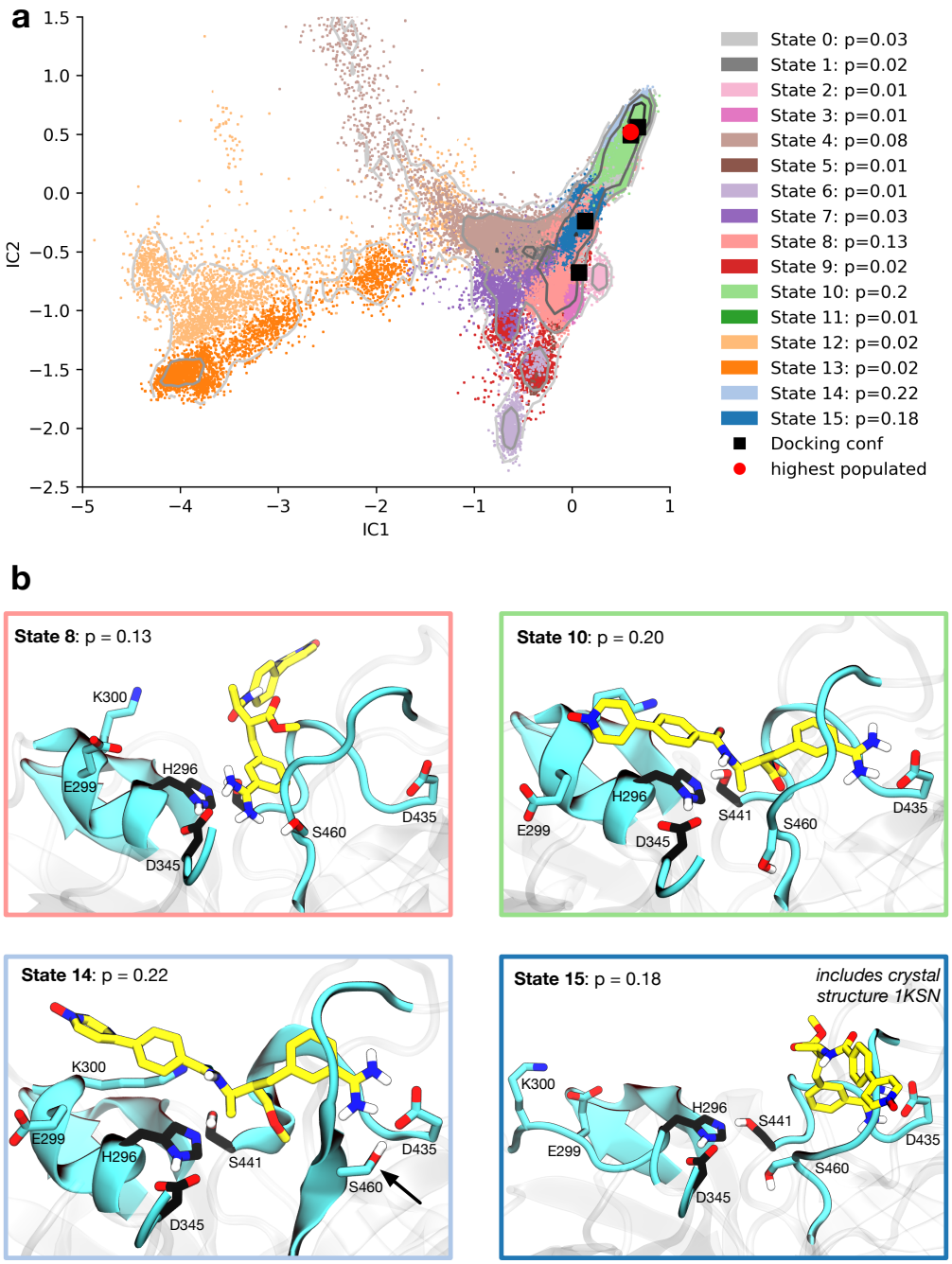

Figure S5: Binding modes of Otamixaban and TMPRSS2. **(a)** Conformational landscape represented by a 2D-VAMP projection of the MD simulation data. We used a 16-state hidden Markov model [4] (HMM) for assigning metastable states (color coded). Reported state probabilities are empirical. Docking configurations that were used for seeding MD simulations are shown as black squares and can be identified with the highest populated states presented below. **(b)** Representative structures for all states with probabilities larger than 10%. Otamixaban is depicted in yellow and catalytic triad in black. States 10 and 14 (different by re-arrangement of S460, cf. black arrow) represent the highest populated binding mode, with a total probability of 42%. State 8 is a pre-bound state with the amidinium head interacting with catalytic triad residues and state 15 represents a binding mode similar to the one found in PDB 1KSN.

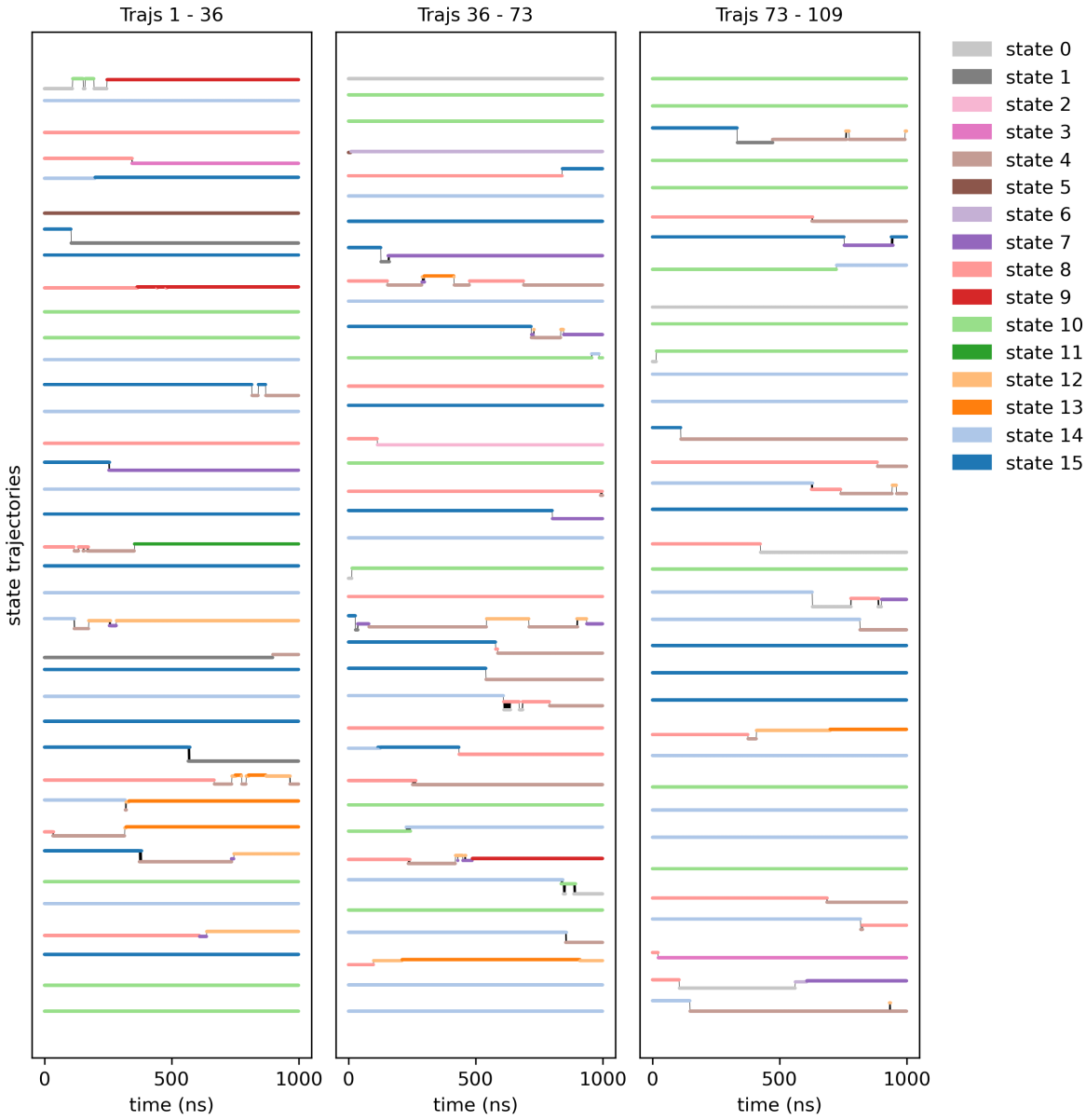

Figure S6: Metastable state trajectories of all MD runs computed from Viterbi paths of HMM states. States and color assignment correspond to results presented in Fig. S5.

References

[1] K. R. Guertin et al. "Optimization of the β-Aminoester class of factor Xa inhibitors. part 2: Identification of FXV673 as a potent and selective inhibitor with excellent In vivo anticoagulant activity". *Bioorganic Med. Chem. Lett.* 12.12 (2002), pp. 1671–1674.

[2] R. C. Edgar. "MUSCLE: Multiple Sequence Alignment with High Accuracy and High Throughput". *Nucleic Acids Research* 32.5 (2004), pp. 1792–1797.

[3] M. Larkin et al. "Clustal W and Clustal X Version 2.0". *Bioinformatics* 23.21 (2007), pp. 2947–2948.

[4] F. Noé, H. Wu, J.-H. Prinz, and N. Plattner. "Projected and Hidden Markov Models for Calculating Kinetics and Metastable States of Complex Molecules". *J. Chem. Phys.* 139.18 (2013), p. 184114.